

Distribution Function for Large Velocities of a Two-Dimensional Gas Under Shear Flow

J. M. Montanero,¹ A. Santos,² and V. Garzó²

Received December 10, 1996; final April 3, 1997

The high-velocity distribution of a two-dimensional dilute gas of Maxwell molecules under uniform shear flow is studied. First we analyze the shear-rate dependence of the eigenvalues governing the time evolution of the velocity moments derived from the Boltzmann equation. As in the three-dimensional case discussed by us previously, all the moments of degree $k \geq 4$ diverge for shear rates larger than a critical value $a_c^{(k)}$, which behaves for large k as $a_c^{(k)} \sim k^{-1}$. This divergence is consistent with an algebraic tail of the form $f(V) \sim V^{-4-\sigma(a)}$, where σ is a decreasing function of the shear rate. This expectation is confirmed by a Monte Carlo simulation of the Boltzmann equation far from equilibrium.

KEY WORDS: Boltzmann equation; velocity moments; Maxwell molecules; uniform shear flow; DSMC method.

I. INTRODUCTION

A difficult and interesting physical problem concerns the high-velocity distribution in a gas far from equilibrium. This information can be obtained indirectly from the knowledge of high-degree velocity moments, but even this represents a formidable task. In addition, the high-velocity distribution is expected to depend on the particular non-equilibrium state considered. In this paper we will study this problem in the case of the so-called uniform shear flow (USF) state, which is perhaps the simplest inhomogeneous situation arbitrarily far from equilibrium. In the USF state, the only non-zero hydrodynamic gradient is $\partial u_x / \partial y = a$, where $\mathbf{u}(\mathbf{r})$ is the flow velocity and a is the *constant* shear rate.

¹ Departamento de Electrónica e Ingeniería Electromecánica, Universidad de Extremadura, E-06071 Badajoz, Spain.

² Departamento de Física, Universidad de Extremadura, E-06071 Badajoz, Spain.

Long time ago, Ikenberry and Truesdell⁽¹⁾ showed that the infinite hierarchy of moment equations obtained from the Boltzmann equation for Maxwell molecules⁽²⁾ can be recursively solved in the case of the USF. In particular, they obtained explicit expressions for the second-degree moments, which are related to the rheological properties, as nonlinear functions of the shear rate. More recently, explicit expressions for the fourth-degree moments have also been derived.⁽³⁾ While the second-degree moments remain finite for arbitrary shear rates, there exists a critical value $a_c^{(4)}$ of the shear rate, beyond which the fourth-degree moments diverge.^(3,4) The analysis of this singular behavior for moments of degree through $k=36$ has been carried out in ref. 5. The results are exact and show that all the moments of the same degree $k \geq 4$ are divergent if the shear rate is larger than a certain critical value $a_c^{(k)}$. The set of critical values $\{a_c^{(4)}, a_c^{(6)}, \dots, a_c^{(36)}\}$ is decreasing and an extrapolation for larger values of k suggests that $a_c^{(k)} \sim k^{-1}$, so that there is no lower bound of $a_c^{(k)}$. This behavior of the moments seems to indicate that the distribution function presents an algebraic high-velocity tail for any value of the shear rate. To the best of our knowledge, however, a confirmation of the above expectation has not been presented.

The aim of this paper is to investigate this problem in the two-dimensional case. Since the geometry of the USF is essentially bidimensional, this allows us to get more detailed information without missing the relevant physical aspects. In Section II we derive the hierarchy of moment equations from the Boltzmann equation for Maxwell molecules. It is shown again that the moments exhibit the same kind of behavior as in the three-dimensional case, but now the analysis has been extended up to $k=240$. The expected algebraic tail of the velocity distribution $f(\mathbf{V})$ is confirmed in Section III by means of the direct simulation Monte Carlo (DSMC) method for solving the Boltzmann equation.⁽⁶⁾ More specifically, the results show that $f(\mathbf{V}) \sim V^{-4-\sigma(a)}$ where $\sigma(a)$ is a decreasing function of the shear rate. Finally, the results are discussed in Section IV.

II. VELOCITY MOMENTS

In the USF state, the velocity distribution function $f(\mathbf{r}, \mathbf{v}, t)$ becomes spatially homogeneous when the velocities are referred to the flow velocity $\mathbf{u}(\mathbf{r}) = ay\hat{\mathbf{x}}$, i.e., $f(\mathbf{r}, \mathbf{v}, t) = f(\mathbf{V}, t)$, where $\mathbf{V} = \mathbf{v} - \mathbf{u}$. Consequently, the Boltzmann equation can be written as⁽³⁾

$$\frac{\partial}{\partial t} f - aV_y \frac{\partial}{\partial V_x} f = \int d\mathbf{V}_1 \int d\hat{\mathbf{n}} B(g, \cos \chi) (f'f'_1 - ff_1) \equiv J[f, f] \quad (2.1)$$

where $J[f, f]$ is the nonlinear Boltzmann collision operator.⁽⁷⁾ Here, $\mathbf{g} = \mathbf{V} - \mathbf{V}_1$, $\hat{\mathbf{n}}$ is a unit vector along the direction of the post-collisional relative velocity, and $\cos \chi = \hat{\mathbf{n}} \cdot \hat{\mathbf{g}}$. The second term on the left-hand side of Eq. (2.1) represents an inertial force. In the absence of a thermostat, the temperature T grows with time, so that the USF is not stationary. The heating equation is

$$nk_B \frac{d}{dt} T = -aP_{xy} \tag{2.2}$$

where n is the constant number density, k_B is the Boltzmann constant, $nk_B T = \frac{1}{2} \text{tr } \mathbf{P}$, and \mathbf{P} is the pressure tensor, defined as

$$P_{ij} = m \int d\mathbf{V} V_i V_j f \tag{2.3}$$

m being the mass of a particle. In Eq. (2.2) and in the definition of T we have considered the case of a two-dimensional system. Henceforth, this will be the case under consideration. In the particular case of Maxwell molecules,⁽⁸⁾ i.e., particles interacting via a repulsive potential of the form r^{-2} , the collision rate B does not depend on the magnitude of the relative velocity \mathbf{g} of the colliding particles. As a consequence, the moments of degree k of the collision operator can be expressed as bilinear combinations of moments of degree equal to or less than k .^(2,9) This property and the simplicity of the USF allows one to get, in principle, the moments in a recursive way. In particular, the elements of the pressure tensor obey a closed set of linear equations.⁽³⁾ Its solution in the long-time limit gives $T(t) \sim e^{2\alpha(a)t}$, where

$$\alpha(a) = \frac{2}{3} v \sinh^2 \left[\frac{1}{6} \cosh^{-1} \left(1 + \frac{27 a^2}{2 v^2} \right) \right] \tag{2.4}$$

In this equation, $v = n\lambda_{02}^0$ is an effective collision frequency, where λ_{02}^0 is an eigenvalue of the linearized Boltzmann operator (c.f. (2.8)).

From a physical point of view, it is interesting to scale velocities with respect to the thermal velocity $v_0(t) = \sqrt{2k_B T(t)/m}$. Thus, we make the changes $\mathbf{V} \rightarrow \mathbf{V}/v_0$, $f \rightarrow v_0^2 f$ and Eq. (2.1) (for Maxwell molecules) becomes

$$\frac{\partial}{\partial t} f - aV_y \frac{\partial}{\partial V_x} f - \alpha \frac{\partial}{\partial \mathbf{V}} \cdot \mathbf{V} f = J[f, f] \tag{2.5}$$

It is worth to remark that Eq. (2.5) is the same as the one corresponding to the USF state in the presence of a thermostat force of the form $-m\alpha\mathbf{V}$.⁽¹⁰⁾ This equivalence holds only for Maxwell molecules. The explicit solution of Eq. (2.5) for arbitrary values of the shear rate a is not known.⁽¹¹⁾ In order to get analytical information about the high-velocity behavior of f , we resort to its velocity moments.

Let us introduce the set of polynomials

$$\Psi_{rm}(\mathbf{V}) = \left[\frac{r!}{\pi(r + |m|)!} \right]^{1/2} V^{|m|} L_r^{|m|}(V^2) e^{im\theta} \tag{2.6}$$

where $L_r^{|m|}$ are associated Laguerre polynomials and $\theta = \tan^{-1}(V_y/V_x)$. The set $\{\Psi_{rm}\}$ is orthonormal with the inner product

$$\langle \phi | \psi \rangle = \pi^{-1} \int d\mathbf{V} e^{-V^2} \phi^*(\mathbf{V}) \psi(\mathbf{V}) \tag{2.7}$$

The choice of the set of polynomials (2.6) is motivated by the fact that they are eigenfunctions of the linearized Boltzmann equation for a two-dimensional Maxwell gas.⁽¹²⁾ The corresponding eigenvalues are

$$\lambda_{rm}^0 = \int_0^{2\pi} d\chi B(\cos \chi) \left\{ 1 + \delta_{2r + |m|, 0} - \cos^{2r + |m|} \frac{\chi}{2} \cos \frac{|m|\chi}{2} - \sin^{2r + |m|} \frac{\chi}{2} \cos \left[\frac{|m|\chi}{2} + \pi \left(\frac{3|m|}{2} + 2r \right) \right] \right\} \tag{2.8}$$

We define the moments

$$M_{rm}(t) = \frac{1}{n} \int d\mathbf{V} \Psi_{rm}^*(\mathbf{V}) f(\mathbf{V}, t) \tag{2.9}$$

so that the distribution function can be represented by

$$f(\mathbf{V}) = n\pi^{-1} e^{-V^2} \sum_k M_k(t) \Psi_k(\mathbf{V}) \tag{2.10}$$

where we have used the short-hand notation $k \equiv (r, m)$. Due to the invariance property $f(\mathbf{V}) = f(-\mathbf{V})$ of Eq. (2.5), we can restrict ourselves to the subset $\{\Psi_{rm}\}$ with even values of $2r + |m| \equiv k$. In that case, the number of independent polynomials of degree k is $k + 1$.

Multiplying both sides of Eq. (2.5) by $\Psi_k^*(\mathbf{V})$ and integrating over \mathbf{V} one gets

$$\begin{aligned} \frac{\partial}{\partial t} M_k + a \sum_{k'} \langle \Psi_{k'} | V_y \frac{\partial}{\partial V_x} | \Psi_k \rangle^* M_{k'} + \alpha \sum_{k'} \langle \Psi_{k'} | \mathbf{V} \cdot \frac{\partial}{\partial \mathbf{V}} | \Psi_k \rangle^* M_{k'} \\ = -n\lambda_k^0 + \sum_{k', k''}^\dagger J_{kk'k''} M_{k'} M_{k''} \end{aligned} \tag{2.11}$$

where the dagger in the last summation denotes the constraints $k' + k'' = k$ and $0 < k', k'' < k$, so that it includes only moments of degree less than k . The explicit form of the coefficients $J_{kk'k''}$ will not be needed here. Since the action of the operator $V_i \partial / \partial V_j$ on Ψ_k is a polynomial of degree k , the brackets appearing in Eq. (2.11) vanish unless $k' \leq k$, so that the hierarchy (2.11) can be solved recursively. If the moments of degree $k' < k$ are known, then Eq. (2.11) can be seen as an inhomogeneous linear system of first order differential equations for the moments of degree k . According to this, Eq. (2.11) can be recast into the form

$$\frac{\partial}{\partial t} M_k + \sum_{(k'=k)} \mathcal{L}_{kk'} M_{k'} = N_k \tag{2.12}$$

where N_k denotes the terms in Eq. (2.11) involving moments of degree less than k and, for a given degree k , $\mathcal{L}_{kk'}$, is a $(k + 1) \times (k + 1)$ matrix defined by

$$\mathcal{L}_{kk'} = (n\lambda_k^0 + k\alpha) \delta_{kk'} + a \langle \Psi_{k'} | V_y \frac{\partial}{\partial V_x} | \Psi_k \rangle^* \tag{2.13}$$

Here we have taken into account that (see the Appendix)

$$\langle \Psi_{k'} | \mathbf{V} \cdot \frac{\partial}{\partial \mathbf{V}} | \Psi_k \rangle = k, (k = k') \tag{2.14}$$

In the Appendix it is also shown that, for $2r + |m| = 2r' + |m'|$,

$$\begin{aligned} \langle \Psi_{r'm'} | V_y \frac{\partial}{\partial V_x} | \Psi_{rm} \rangle = \left(S_{rm} \delta_{|m'|, |m|+2} - S_{r'm'} \delta_{|m|, |m'|+2} - \frac{i}{2} |m| \delta_{|m|, |m'|} \right) \\ \times [H(m) H(m') - H(-m) H(-m')] \end{aligned} \tag{2.15}$$

where

$$S_{rm} = \frac{i}{2} \sqrt{r(r + |m| + 1)} \tag{2.16}$$

and H is Heaviside's step function, i.e., $H(x) = 1$ if $x \geq 0$, being 0 otherwise.

It is important to emphasize that Eq. (2.12) holds for *any* value of the shear rate. In fact, the matrix $\mathcal{L}_{kk'}$, depends on a both explicitly and through $\alpha(a)$. To clarify the subsequent analysis, let us assume that the shear rate is such that the moments of degree $k' < k$ have reached stationary values. Thus, the time behavior of M_k is given by the eigenvalues $\lambda_k(a)$ of $\mathcal{L}_{kk'}$; obviously, $\lambda_k(0) = \lambda_k^0$. For long times, the behavior is governed by the eigenvalue with the smallest real part, $\tilde{\lambda}_k(a)$. If $\text{Re } \tilde{\lambda}_k(a) > 0$, then all the moments of degree k attain stationary values; otherwise, they grow exponentially in time. We have obtained the eigenvalues $\lambda_k(a)$ from $k = 4$ through $k = 240$. For the sake of illustration, we have considered the case of isotropic scattering,⁽¹²⁾ i.e., $B(\cos \chi) = \text{const}$. In that case, $v = n\lambda_{02}^0 = \pi nB$. Hereafter, we take v^{-1} as the unit of time and we also take $\lambda_{02}^0 = 1$. As happens in the three-dimensional case,⁽⁵⁾ we have found that $\tilde{\lambda}_k$ turns out to be $\lambda_{(k/2)0}$, is a real number, and monotonically decreases as the shear rate increases. Eventually, $\lambda_{(k/2)0}$ becomes negative for shear rates larger than a certain critical value $a_c^{(k)}$. As an example, Fig. 1 shows the shear-rate

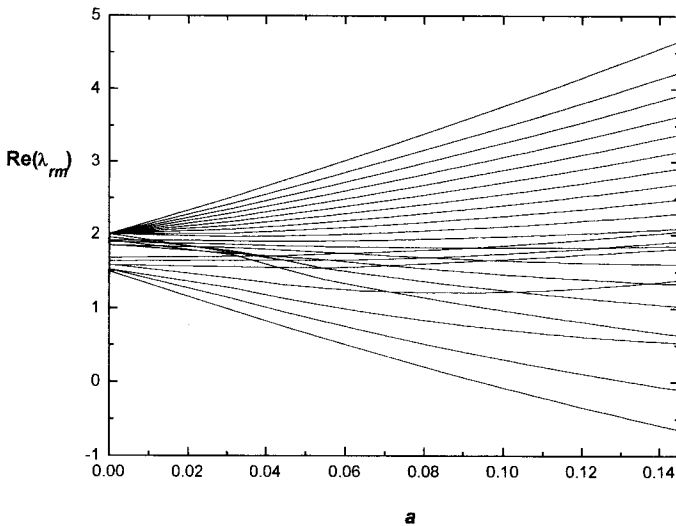


Fig. 1. Shear-rate dependence of the real part of the eigenvalues corresponding to the moments of degree $2r + |m| = 40$.

dependence of the real part of the eigenvalues corresponding to degree $k = 40$. The smallest eigenvalue, $\tilde{\lambda}_{40} = \lambda_{20,0}$, becomes negative if $a > a_c^{(40)} \simeq 0.094$. It is interesting to remark that the degeneracy of the eigenvalues at equilibrium is broken; in particular, both $\lambda_{19,2}^0$ and $\lambda_{18,4}^0$ degenerate in a pair of real eigenvalues. The value of the critical shear rate $a_c^{(k)}$, beyond which the moments of degree k diverge, decreases as k increases. For instance, $a_c^{(240)} \simeq 0.016$.

From a practical point of view, we have determined $a_c^{(k)}$ as the smallest real root of $\Delta_k(a) = 0$, where $\Delta_k \equiv \det \mathcal{L}_{kk}$. The results are represented in Fig. 2 as a log-log plot. The points corresponding to large values of k tend to align with a slope practically equal to -1 . Consequently, we can conclude that there is no lower bound of the set $\{a_c^{(k)}\}$, i.e., $\lim_{k \rightarrow \infty} a_c^{(k)} = 0$. This means that, no matter how small the shear rate is, there is always an infinite number of diverging moments. In addition, the asymptotic behavior for large k is of the form $a_c^{(k)} \approx \bar{a}_c k^{-1}$, the coefficient being $\bar{a}_c \simeq 3.8$. This suggests that a certain scaling might exist for large values of k . This is confirmed by Fig. 3, where the scaled determinant $F_k(\bar{a}) = \Delta_k(a) / \Delta_k(0)$ is plotted versus the scaled shear rate $\bar{a} = ka$ for $k = 12, 30, 74, 150$, and 220 . We see that, as k increases, $F_k(\bar{a})$ tends to a common curve with a zero at $\bar{a} = \bar{a}_c$. It is interesting to note that the asymptotic behavior $a_c^{(k)} \sim k^{-1}$ is consistent with the results obtained in ref. 5 for a three-dimensional system with both the actual and the isotropic scattering. This suggests that this behavior is independent of the dimensionality and the details of the scattering law (for Maxwell molecules). We have confirmed the latter conclusion by considering the highly anisotropic

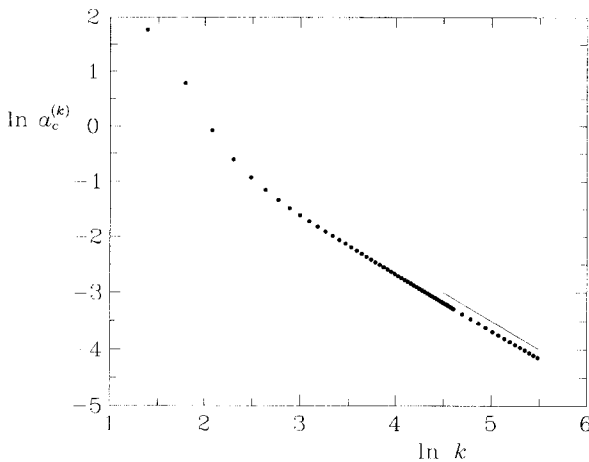


Fig. 2. Log-log plot of $a_c^{(k)}$ versus k . The straight line has a slope equal to -1 .

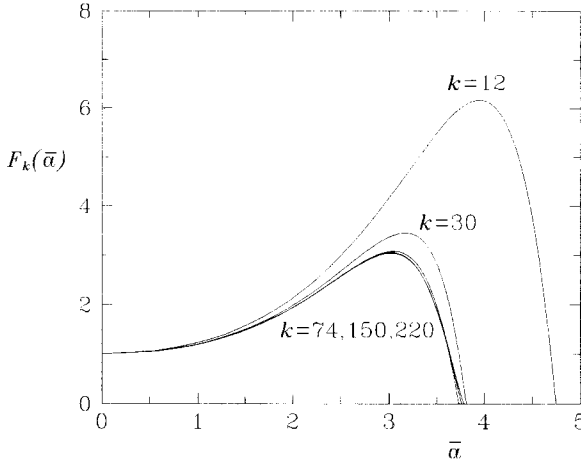


Fig. 3. Scaled determinant $F_k(\bar{a}) = A_k(a)/A_k(0)$ as a function of the scaled shear rate $\bar{a} = ka$ for $k = 12, 30, 74, 150$ and 220 .

scattering law $B(\cos \chi) \propto \delta(\chi - (\pi/2))$. Again, we get $a_c^{(k)} \approx \bar{a}_c k^{-1}$ with practically the same value of the coefficient \bar{a}_c .

A natural question is, what information about the high-velocity distribution can be drawn out from this singular behavior of the moments? The simplest possibility is that a stationary solution of Eq. (2.5) does exist, but with an algebraic tail of the form $f \sim V^{-4-\sigma}$. In that case, all the moments of degree equal to or larger than $2 + \sigma$ would be divergent. This scenario is consistent with our analysis of the moments if σ is a decreasing function of the shear rate, the critical values $a_c^{(k)}$ being then the values at which $\sigma(a)$ takes integer values $k - 2$. Furthermore, σ goes to infinity as the shear rate tends to zero according to the law $\sigma \approx \bar{a}_c a^{-1}$. Since the moments of degree 2 are convergent for any value of the shear rate, σ must be positive. We have not been able to prove the above conjectures from an exact analysis of Eq. (2.5). Alternatively, we have resorted to a numerical solution and the results are presented in the next Section.

III. MONTE CARLO SIMULATION

A highly reliable numerical algorithm to solve the Boltzmann equation is the so-called direct simulation Monte Carlo (DSMC) method.⁽⁶⁾ Its application to USF has been validated in several works.^(13, 14) Since the problem is spatially homogeneous (in the Lagrangian frame), only the

velocities \mathbf{V}_i , $i = 1, \dots, N$ of a “system” of N particles need to be stored. At times $t = \Delta t, 2 \Delta t, \dots$, where Δt is a time-step much smaller than the mean free time, the velocities are updated due to (i) collisions and (ii) external forces: $\{\mathbf{V}_i\} \xrightarrow{(i)} \{\mathbf{V}'_i\} \xrightarrow{(ii)} \{\mathbf{V}''_i\}$. According to the Boltzmann collision term for isotropic Maxwell molecules, the average number of particles that change their velocities due to collisions during an interval Δt must be $(2\pi nB) N \Delta t$. Consequently, in the simulations a number $\nu N \Delta t$ of pairs is chosen at random. For each pair (i, j) , a direction $\hat{\mathbf{n}}$ is taken at random with equiprobability and the velocities are changed to

$$\mathbf{V}'_i = \frac{1}{2}(\mathbf{V}_i + \mathbf{V}_j) + \frac{1}{2} \mathbf{g} \hat{\mathbf{n}}, \quad \mathbf{V}'_j = \frac{1}{2}(\mathbf{V}_i + \mathbf{V}_j) - \frac{1}{2} \mathbf{g} \hat{\mathbf{n}} \quad (3.1)$$

where $\mathbf{g} = \mathbf{V}_i - \mathbf{V}_j$. For non-colliding particles, $\mathbf{V}'_i = \mathbf{V}_i$. Once the collision stage ends, the velocities are changed due to the action of the inertial force and the thermostat:

$$\mathbf{V}''_i = e^{-\alpha \Delta t} (\mathbf{V}'_i - \mathbf{a} \cdot \mathbf{V}'_i \Delta t) \quad (3.2)$$

where the elements of the tensor \mathbf{a} are $a_{ij} = a \delta_{ix} \delta_{jy}$.

In order to analyze the distribution function for high velocities, it is convenient to focus on the magnitude of the velocities and to define $\Phi(V) = n^{-1} \int d\hat{\mathbf{V}} V f(\mathbf{V})$. In the simulations, this quantity is obtained as

$$\Phi(V) = \frac{1}{N \Delta V} \sum_{i=1}^N H\left(V_i - V + \frac{1}{2} \Delta V\right) H\left(-V_i + V + \frac{1}{2} \Delta V\right) \quad (3.3)$$

We have taken $N = 10^4$, $\Delta t = 0.001$, and $\Delta V = 0.04$. To improve the statistics, the results have been averaged over a number \mathcal{N} of different replicas.

According to the conjecture stated at the end of Sect. II, the behavior of Φ for large V is

$$\Phi(V) \sim V^{-3 - \sigma(a)}, \quad (3.4)$$

where $\sigma(a_c^{(k)}) = k - 2$. Figure 4 shows the time evolution of $V^5 \Phi(V)$ for $V = 11.6$ and $V = 13.3$ at $a = a_c^{(4)} \simeq 5.847$. The number of replicas has been $\mathcal{N} = 5000$ and the initial condition has been local equilibrium. It is observed that in both cases a *common* stationary value is reached after a transient period of $t \approx 20$, which is about 10 times the relaxation time of the second-degree moments. As a measure of how far the system is from equilibrium at $a \simeq 5.847$, it is interesting to remark that, at equilibrium,

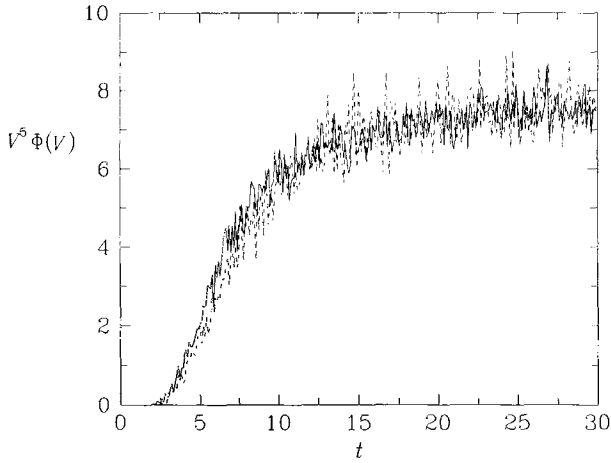


Fig. 4. Time evolution of $V^5\Phi(V)$ for $V=11.6$ (solid line) and $V=13.3$ (dashed line). The shear rate considered is $a=a_c^{(4)} \simeq 5.847$.

$V^5\Phi(V) \sim 10^{-52}$ at $V=11.6$ and $V^5\Phi(V) \sim 10^{-70}$ at $V=13.3$. We have verified that the behavior found in Fig. 4 extends to higher velocities; of course, the statistical fluctuations increase considerably as the velocity increases. This is shown in Fig. 5, where the scaled distribution $V^5\Phi(V)$, averaged over the time interval $15 < t < 20$ and with $\mathcal{N} = 600$, is plotted versus V . This quantity reaches a value independent of the velocity for $V \gtrsim 10$.

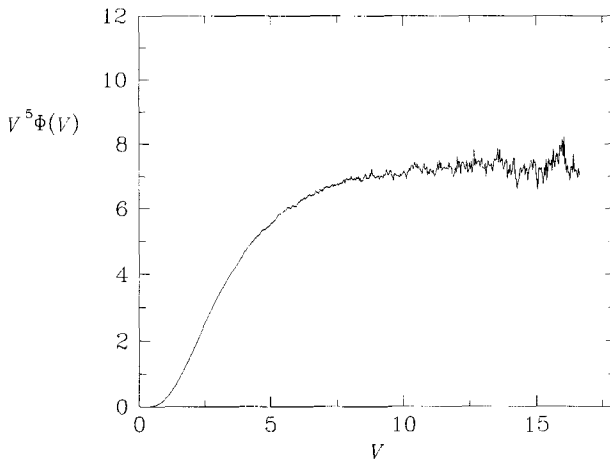


Fig. 5. Plot of $V^5\Phi(V)$ for $a=a_c^{(4)} \simeq 5.847$.

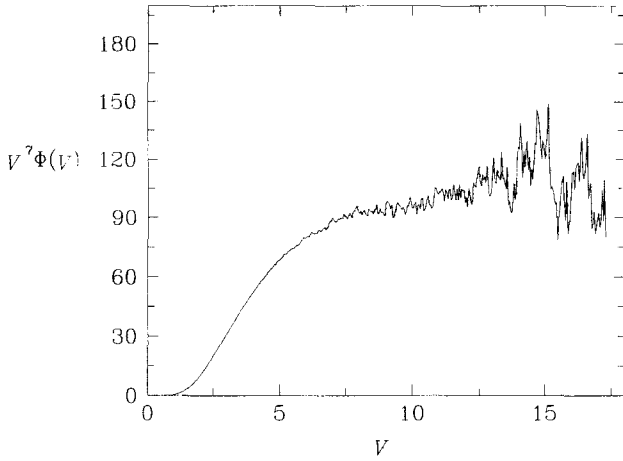


Fig. 6. Plot of $V^7\phi(V)$ for $a = a_c^{(6)} \simeq 2.196$.

We have also considered the shear rate $a = a_c^{(6)} \simeq 2.196$. In this case, the relaxation time of the distribution tail is longer than the one with the previous shear rate. Now, $V^7\phi(V)$ must reach a constant value, as shown in Fig. 6, where the values have been averaged over $45 < t < 60$ with $\mathcal{N} = 500$. Since now the high-velocity population is smaller than before, the fluctuations have increased significantly.

So far, we have chosen values of the shear rate at which σ takes integer values. For other values of a , σ cannot be inferred from the

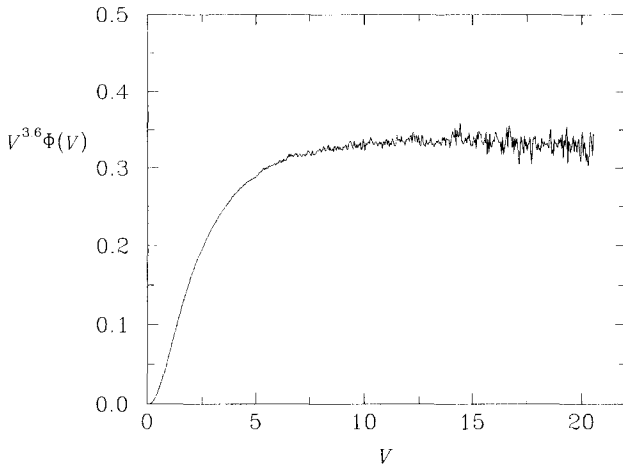


Fig. 7. Plot of $V^{3.6}\phi(V)$ for $a = 12$.

knowledge of the singular behavior of the moments. In that case, σ must be obtained empirically from the slope of a log-log plot of Φ versus V for long times and large velocities. In this way, we have obtained $\sigma \simeq 1.4$ for $a = 8$ and $\sigma \simeq 0.6$ for $a = 12$. The latter case is represented in Fig. 7, where we have averaged over $15 < t < 20$ with $\mathcal{N} = 200$. Since σ decreases significantly as the shear rate increases, it is tempting to speculate that $\lim_{a \rightarrow \infty} \sigma(a) = 0$. Of course, σ cannot be negative since the second-degree moments are finite for any shear rate.

To complete our knowledge about the distribution function $f(\mathbf{V})$, we have analyzed its dependence on the direction $\hat{\mathbf{V}}$ in the high-energy region. We have found that this dependence is the same for all the values of V , so that $f(\mathbf{V}) \approx nV^{-1}\Phi(V)\Theta(\theta)$. Thus, $\Theta(\theta)d\theta$ is the probability of finding a particle with a polar angle between θ and $\theta + d\theta$ in the high-energy region. Figure 8 shows a polar diagram of the function $\Theta(\theta)$ for $a = a_c^{(4)} \simeq 5.847$, $a = 8$, and $a = 12$. It is clear that this distribution is highly anisotropic, although the characteristic symmetry of the USF, namely $\Theta(\theta) = \Theta(\theta + \pi)$ is preserved. Most of the particles move along directions almost parallel to the x -axis, which is the direction of the inertial force. This effect is more significant as the shear rate increases.

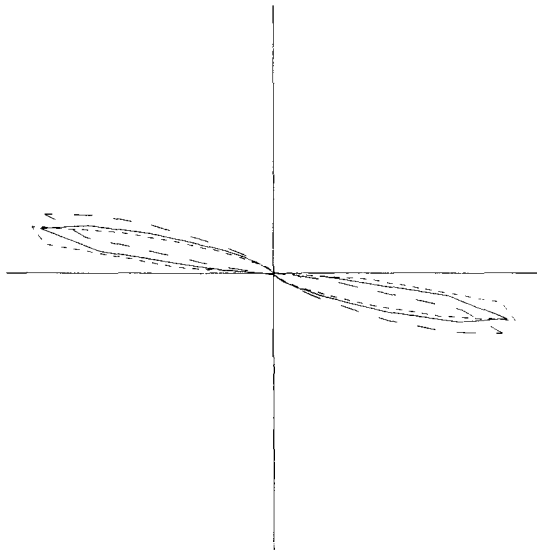


Fig. 8. Polar diagram of the function $\Theta(\theta)$, evaluated in the region $V > 11.5$, for $a = a_c^{(4)} \simeq 5.847$ (---), $a = 8$ (—), and $a = 12$ (-·-·-).

IV. CONCLUSIONS

In this paper we have analyzed the high-velocity distribution of a two-dimensional dilute gas of Maxwell molecules described by the Boltzmann equation, under uniform shear flow. This state, in which the only non-equilibrium control parameter is the constant shear rate a , is one of the most widely studied in several statistical-mechanical problems, such as nonlinear transport⁽¹⁵⁾ or the relationship with chaotic dynamics.⁽¹⁶⁾ Two complementary approaches have been followed: (i) an exact analysis of the hierarchy of moment equations and (ii) a numerical evaluation of the velocity distribution function by means of the DSMC method. Both routes lead to the conclusion that the stationary velocity distribution develops an algebraic high-velocity tail of the form $f(\mathbf{V}; a) \approx C(a) V^{-4-\sigma(a)} \Theta(\hat{\mathbf{V}}; a)$. For a d -dimensional system, the behavior would be⁽¹⁷⁾ $f \sim V^{-d-2-\sigma}$. The exponent $\sigma(a)$ is a decreasing function of the shear rate with the properties $\sigma \sim a^{-1}$ for small a and $\lim_{a \rightarrow \infty} \sigma = 0$. While we have not been able to get an explicit expression for $\sigma(a)$, the analysis of the moments carried out in Sect. II provides a wealth of information about it. In particular, Fig. 2 can be interpreted as showing $\sigma(a)$ by making the changes $k \rightarrow \sigma + 2$ and $a_c^{(k)} \rightarrow a$. The polar distribution Θ indicates that most of the energetic particles tend to move, relative to the local velocity, along a narrow interval of directions, which are quasi-parallel to the flow direction. Regarding the amplitude $C(a)$, from Figs. 5–7 one can conclude that it increases as the shear rate decreases. The fact that the algebraic tail persists even for very small shear rates implies that the population of particles with large velocities can be very different from that of equilibrium. As a consequence, those phenomena in which that population plays an important role may not be well described by perturbation techniques, such as the Chapman–Enskog expansion.⁽⁹⁾

Although we have restricted here to the Maxwell interaction, a DSMC investigation of the time evolution of the velocity moments for other repulsive interactions⁽¹⁴⁾ suggests that the above singular behavior is also present in those cases. The main influence of the interaction is that, for a given value of the shear rate in appropriate dimensionless units, the exponent σ is larger as the repulsion becomes harder. In particular, in the limit of hard spheres, σ is probably infinity, so that the algebraic tail disappears.

The simplicity of the uniform shear flow state has allowed us to offer a thorough analysis of the nonequilibrium population of particles with large velocities. Nevertheless, we expect that some of the features found here might be extended to other nonequilibrium situations as well.

APPENDIX

Here the equalities (2.14) and (2.15) are proved. First we list the properties of the Laguerre polynomials⁽¹⁸⁾ that will be used:

$$x \frac{d}{dx} L_r^{[m]}(x) = r L_r^{[m]}(x) - (r + |m|) L_{r-1}^{[m]}(x) \tag{A1}$$

$$x L_r^{[m]}(x) = -(r + 1) L_{r+1}^{[m]}(x) + (2r + |m| + 1) L_r^{[m]}(x) - (r + |m|) L_{r-1}^{[m]}(x), \tag{A2}$$

$$\frac{d}{dx} L_r^{[m]}(x) = -L_{r-1}^{[m]+1}(x) \tag{A3}$$

$$\int_0^\infty dx e^{-x} x^{|m|} L_r^{[m]}(x) L_{r'}^{[m]}(x) = \begin{cases} 0, & r' < r \\ C_{rm}, & r' = r \end{cases} \tag{A4}$$

where $C_{rm} \equiv (r + |m|)!/r!$

We note that $\mathbf{V} \cdot \partial/\partial \mathbf{V} = V \partial/\partial V$. Thus

$$\mathbf{V} \cdot \frac{\partial}{\partial \mathbf{V}} \Psi_{rm} = (2r + |m|) \Psi_{rm} - 2 \sqrt{r(r + |m|)} \Psi_{r-1, m} \tag{A5}$$

where use has been made of the recurrence relation (A1). Equation (2.14) easily follows from Eq. (A5).

Now, we consider the equality

$$\begin{aligned} V_y \frac{\partial}{\partial V_x} &= \sin \theta \cos \theta V \frac{\partial}{\partial V} - \sin^2 \theta \frac{\partial}{\partial \theta} \\ &\equiv A_V - A_\theta \end{aligned} \tag{A6}$$

Let us consider first the matrix elements of the operator A_V :

$$\begin{aligned} \langle \Psi_{r'm'} | A_V | \Psi_{rm} \rangle &= \frac{i}{2 \sqrt{C_{r'm'} C_{rm}}} (\delta_{m', m-2} - \delta_{m', m+2}) \\ &\times \int_0^\infty dx e^{-x} x^{|m'|/2} L_{r'}^{[m']}(x) x \frac{d}{dx} [x^{|m|/2} L_r^{[m]}(x)] \end{aligned} \tag{A7}$$

Since we are interested in the case $2r + |m| = 2r' + |m'|$, we only need to consider in the integral over x the cases $r' = r \pm 1$. If $r' = r + 1$, one has

$$\int_0^\infty dx e^{-x} x^{|m|/2-1} L_{r+1}^{|m|-2}(x) x \frac{d}{dx} [x^{|m|/2} L_r^{|m|}(x)] = -r(r+1) C_{r+1, |m|-2} - \frac{(r+1)|m|}{2} C_{r+1, |m|-2} \quad (A8)$$

where use has been made of Eqs. (A1)–(A4). Analogously, if $r' = r - 1$, one has

$$\int_0^\infty dx e^{-x} x^{|m|/2+1} L_{r-1}^{|m|+2}(x) x \frac{d}{dx} [x^{|m|/2} L_r^{|m|}(x)] = -C_{r-1, |m|+2} - \frac{r|m|}{2} C_{rm} \quad (A9)$$

The matrix elements of the operator A_θ are

$$\langle \Psi_{r'm'} | A_\theta | \Psi_{rm} \rangle = \frac{i}{2\sqrt{C_{r'm'} C_{rm}}} m(\delta_{m', m-2} + \delta_{m', m+2} - 2\delta_{m'm}) \times \frac{1}{2} \int_0^\infty dx e^{-x} x^{|m|/2} L_{r'}^{|m|}(x) x^{|m|/2} L_r^{|m|}(x) \quad (A10)$$

We need to evaluate the integral over x in the cases $r' = r, r \pm 1$. If $r' = r$, then

$$\int_0^\infty dx e^{-x} x^{|m|} L_r^{|m|}(x) L_r^{|m|}(x) = C_{rm} \quad (A11)$$

If $r' = r + 1$,

$$\int_0^\infty dx e^{-x} x^{|m|-1} L_{r+1}^{|m|}(x) L_{r+1}^{|m|-2}(x) = -(r+1) C_{r+1, |m|-2} \quad (A12)$$

Finally, if $r' = r - 1$,

$$\int_0^\infty dx e^{-x} x^{|m|+1} L_{r-1}^{|m|}(x) L_{r-1}^{|m|+2}(x) = -r C_{rm} \quad (A13)$$

Putting together all the results, and after some algebra, one gets Eq. (2.15).

ACKNOWLEDGMENTS

This research was supported by the DGICYT (Spain) and by the Junta de Extremadura (Fondo Social Europeo) through grants PB94-1021 and EIA-39, respectively.

REFERENCES

1. E. Ikenberry and C. Truesdell, On the pressures and the flux of energy in a gas according to Maxwell's kinetic theory. I, *J. Rat. Mech. Anal.* **5**:1–54 (1956); C. Truesdell, On the pressures and the flux of energy in a gas according to Maxwell's kinetic theory. II, *J. Rat. Mech. Anal.* **5**:55–128 (1956).
2. C. Truesdell and R. G. Muncaster, *Fundamentals of Maxwell's kinetic theory of a simple monatomic gas* (Academic Press, New York, 1980).
3. A. Santos and V. Garzó, Exact moment solution of the Boltzmann equation for uniform shear flow, *Physica A* **213**:409–425 (1995).
4. A. Santos, V. Garzó, J. J. Brey, and J. W. Dufty, Singular behavior of shear flow far from equilibrium, *Phys. Rev. Lett.* **71**:3971–3974 (1993); **72**:1392 (Erratum) (1994).
5. J. M. Montanero, A. Santos and V. Garzó, Singular behavior of the velocity moments of a dilute gas under uniform shear flow, *Phys. Rev. E* **53**:1269–1272 (1996).
6. G. A. Bird, *Molecular gas dynamics and the direct simulation of gas flows* (Clarendon, Oxford, 1994).
7. R. Dorfman and H. van Beijeren, The kinetic theory of gases, in *Statistical Mechanics. Part B: Time-dependent processes*, B. J. Berne, ed. (Plenum Press, New York, 1977), pp. 65–179.
8. M. H. Ernst, Nonlinear model-Boltzmann equations and exact solutions, *Phys. Rep.* **78**:1–171 (1981).
9. J. A. McLennan, *Introduction to Nonequilibrium Statistical Mechanics* (Prentice-Hall, Englewood Cliffs, NJ, 1989).
10. D. J. Evans and G. P. Morriss, *Statistical Mechanics of Nonequilibrium Liquids* (Academic Press, London, 1990).
11. For a perturbation solution through order a^3 in the three-dimensional case, see J. M. Montanero and A. Santos, Nonequilibrium entropy of a sheared gas, *Physica A* **225**:7–18 (1996).
12. E. M. Hendriks and T. M. Nieuwenhuizen, Solution to the nonlinear Boltzmann equation for Maxwell models for nonisotropic initial conditions, *J. Stat. Phys.* **29**:591–615 (1982). Notice a misprint in Eq. (2.16).
13. J. Gómez Ordóñez, J. J. Brey, and A. Santos, Shear-rate dependence of the viscosity for dilute gases, *Phys. Rev. A* **39**:3038–3040 (1989); J. M. Montanero and A. Santos, Comparison of the DSMC method with an exact solution of the Boltzmann equation, in *Rarefied Gas dynamics*, J. Harvey and G. Lord, eds. (Oxford University Press, Oxford, 1995), pp. 899–905; C. Cercignani and S. Cortese, Validation of a Monte Carlo simulation of the plane Couette flow of a rarefied gas, *J. Stat. Phys.* **75**:817–838 (1994).
14. J. M. Montanero, A. Santos, and V. Garzó, Monte Carlo simulation of the Boltzmann equation for uniform shear flow, *Phys. Fluids* **8**:1981–1983 (1996).
15. *Nonlinear Fluid Behavior*, H. J. M. Hanley, ed. (North-Holland, Amsterdam, 1983).

16. *The Microscopic Approach to Complexity by Molecular Simulations*, M. Mareschal and B. L. Holian, eds. *Physica A* **240**(1-2) (1997).
17. J. M. Montanero, V. Garzó, and A. Santos, High-velocity tail in a dilute gas under shear, in *Rarefied Gas Dynamics*, C. Shen, ed. (Peking University Press, in press).
18. M. Abramowitz and I. Stegun, *Handbook of Mathematical Functions* (Dover, New York, 1965).